Mechanistic Aspects of Homogeneous and Heterogeneous Melting Processes

Francesco Delogu*

Dipartimento di Ingegneria Chimica e Materiali, Università degli Studi di Cagliari, piazza d'Armi, I-09123 Cagliari, Italy

Received: February 27, 2006; In Final Form: May 9, 2006

Molecular dynamics simulations have been employed to explore the response of crystalline Ar systems with and without a free surface to a gradual temperature rise. The surface-free crystalline bulk undergoes a homogeneous melting process at the limit of superheating, whereas the semicrystal terminating with a free plane surface melts with a heterogeneous mechanism at a temperature corresponding to the equilibrium melting point. Numerical findings suggest that the gradual disordering of the crystalline lattice as well as the homogeneous and heterogeneous melting processes are mediated by atoms with defective coordination. Their concentration in the regions close to the semicrystal surface at the equilibrium melting point is found to be approximately the same as in the surface-free bulk at the limit of superheating.

I. Introduction

Melting can be defined as the transition from an ordered crystalline phase with vibrational modes only to a disordered liquid phase within which vibrational and translational modes coexist[1]. The transition behavior is a consequence of structural instabilities governed by thermodynamic quantities[1]. The onset of melting involves either the heterogeneous nucleation of the molten phase at lattice defects or its homogeneous nucleation in the bulk once that thermodynamic melting has been suppressed.[1−12] In the latter case, the lattice stability is limited by a hierarchy of internal energy-,[13] enthalpy-, entropy-, and volume-driven catastrophes.[14] The first limit to the crystal stability is of kinetic nature and the corresponding melting process initiates in excited bulk regions in which large-amplitude thermal vibrations induce a local failure of the crystal.[10−12]

Despite the constant advances in the field, a comprehensive theoretical framework able to rationalize the atomistic processes governing the different transition behaviors is still lacking[1]. Such framework is available only for two-dimensional systems, for which the key role played by lattice defects has been ascertained and the route to structural disorder described as a sequence of defect-mediated processes involving two continuous transitions.[15−17] The disassociation of dislocations leads first to the loss of the translational order and the formation of an intermediate hexatic phase retaining orientational order. Successively, the generation of disclinations determines the loss of the residual orientational order and the final transition to the liquid.[15−17] The positive evidences[18−21] currently supporting the so-called KTHNY mechanism encourage its extension to melting processes in three-dimensional systems.[22−24] Unfortunately, such extension gives rise to serious difficulties even though the topological defects responsible for the breakdown of crystalline order have been already identified with thermally excited dislocation lines.[22−24] In the attempt of giving a contribution along this line of inquiry, this work investigates the role of lattice defects in heterogeneous and homogeneous melting processes by means of numerical simulations. It, therefore, represents an ideal continuation of previous studies[11,12] suggesting the existence of a definite connection between homogeneous and heterogeneous melting scenarios. Taking advantage of previous inferences concerning the similar dynamic properties of bulk and surface atoms respectively at the homogeneous melting point and at the much lower equilibrium one, the present investigation is indeed aimed to characterize the common aspects shared by the different melting processes. To this end, the atomic-scale mechanistic features of the solid−liquid transitions taking place under different thermodynamic conditions are here compared by exploring the coordination number of each atom.[9,24] Attention is focused in particular on the behavior of atoms in layers close to the free surface at the equilibrium melting point and in a bulk system at the limit of superheating.

II. Computational Methods

Molecular dynamics (MD) simulations were performed on systems consisting of 6912 Ar atoms arranged in the face-centered-cubic (fcc) cF4 structure. Systems of 2048 and 10 976 atoms were used to investigate possible size effects. The conventional 12−6 Lennard−Jones (LJ) pair potential was employed to reproduce the interatomic forces.[11] The LJ diameter σ and the energy well depth ϵ were set equal to 0.3405 nm and 1.65×10^{-21} J, respectively. Forces were computed within a cutoff radius equal to 3 σ. Simulations were carried out within the Nosè−Andersen (*NPT*) ensemble with the number of atoms N, the temperature T, and the pressure P constant.[25,26] The Parrinello−Rahman scheme allowing for the change of the shape of the elementary crystallographic cell was also implemented.[27] The equations of motion were solved with a fifth-order predictor−corrector algorithm[28] and a time step δt equal to 2.0 fs. The initial atomic configurations employed to study homogeneous and heterogeneous melting processes were equilibrated for 1×10^5 time steps at a temperature $T = 60$ K and an external pressure $P \approx 0$. The temperature was successively increased by 0.05 K every 2500 time steps, corresponding to a nominal heating rate of 1×10^{10} K s^{-1}. Such heating rate was used in all the simulations discussed in the work.

III. Homogeneous Melting

The homogeneous nucleation of the molten phase in a surface-free bulk of Ar atoms has been already discussed in detail in

* Corresponding author e-mail: delogu@dicm.unica.it.

10.1021/jp061225k CCC: $33.50
Published on Web 06/02/2006

previous works,[29,30] and the methodologies employed to simulate such process, as well as the results obtained, will be here only briefly summarized for sake of clarity.

A surface-free bulk was generated by arranging the 6912 atoms in a cubic simulation box having 12 elementary fcc cF4 cells per side and applying periodic boundary conditions (PBCs)[28] along the three Cartesian directions. The decrease of the long-range order and its disappearance as a consequence of the gradual heating and the successive melting of the crystal were characterized by means of the static order parameter $S(\boldsymbol{k})$.[28] Due to the absence of free surfaces and interfaces, the equilibrium melting is suppressed and the collapse of the crystalline phase, marked by a sudden drop of $S(\boldsymbol{k})$ values, takes place at about 93.5 K[11,29,30]. This temperature represents the first limit of superheating T_m^K.

The fact that the drop of $S(\boldsymbol{k})$ values becomes irreversible when $S(\boldsymbol{k})$ is smaller than 0.6 suggests a rough melting criterion that will be repeatedly employed in the present work. Accordingly, any crystalline region characterized by $S(\boldsymbol{k})$ values smaller than 0.6 will be considered as molten.

Homogeneous melting is mediated by atoms characterized by a coordination number different from twelve, the normal coordination number in a fcc lattice. The number of nearest neighbors was evaluated by means of a distance criterion[24,29,30] according to which two atoms are nearest neighbors when their distance is shorter than the one, r_{min}, corresponding to the first minimum of the pair correlation function (PCF).[28] The identification of a defective atoms relies thus upon the statistical definition of the first coordination shell. Other choices are in principle possible. For example, a local coordination parameter can be used. This however complicates the analysis of atomic configurations without adding any significant insight and the results are essentially the same. The fraction $\alpha_d(T)$ of defective atoms, defined as the ratio between the number of defective atoms and the total number of atoms in the system, increases smoothly with the temperature, assuming at T_m^K a value of about 0.4.[29,30] The formation of defective atoms is strictly connected with the occurrence of thermal atomic vibrations. As the amplitude of thermal vibrations increases, neighboring atoms reciprocally hinder their own motion determining transient atomic strains that induce a local rise of potential energy. Such strains are partially relieved via a local rearrangement of the coordination shells of two nearest neighbors resulting in the appearance of pairs of 11-fold and 13-fold coordinated atoms,[29,30] other defective coordination numbers being rarely observed. It is here worth noting that the formation of pairs of 11- and 13-fold coordinated atoms is reminiscent of the appearance of disclinations in two-dimensional systems[1,15−22]. In a triangular lattice, the thermal disorder produces tightly bound dislocation quadrupoles consisting of two pairs of atoms with 7- and 5-fold coordinated atoms[1,15−22]. The KTHNY scenario relies upon such structural motifs and their gradual disassociation as the amplitude of atomic vibrations increases. Although the situation in three-dimensional systems is remarkably more complex than in two-dimensional ones, the number and the arrangement of defective atoms can however provide significant insight into the melting behavior and permits a comparison between apparently different melting processes. It is within this framework that the fraction $\alpha_d(T)$ of defective atoms and the number N_{cl} of clusters they form will be used in the present study.

The mechanism governing the formation of defective atoms displays a cooperative character that is responsible for the generation of connected structures of defective atoms, the number N_{cl} and size n of which depend on the temperature. These quantities can be evaluated according to the same distance criterion mentioned above[24,29,30], so that two defective atoms belong to the same cluster when their distance is shorter than r_{min}. The clusters, an example of which is depicted in Figure 1 for sake of illustration, have a fractal geometry similar to the one of self-avoiding random walks.[29−31] As the temperature increases, some clusters display properties characteristic of dislocation lines and loops. In particular, Shockley partial dislocations with a (111) glide plane moving irregularly in the [110] and one of the [211] crystallographic directions have been observed. Small dislocation loops surround sometimes stacking faults, i.e., crystalline domains with the hexagonal-close-packed (hcp) arrangement, pointed out by employing the so-called Honeycutt−Andersen parameters[29,30,32]. No body-centered cubic (bcc) stacking has been detected. Configurations of 12 nearest neighbor atoms with 11-fold as well as with 13-fold coordination, corresponding respectively to individual vacancies and interstitials, have been also observed. Their fractions α_{vac} and α_{int} change with temperature, but remain on the order of 1×10^{-3} at any temperature.

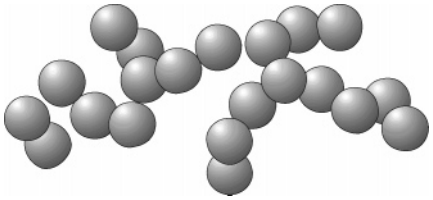

Figure 1. Planar projection of a cluster of 21 defective atoms at 75 K.

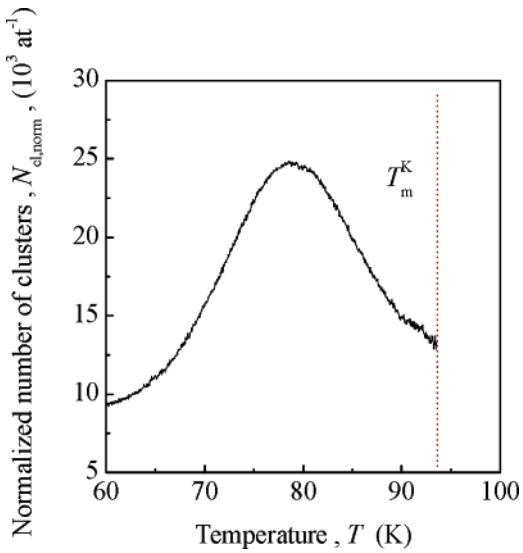

Figure 2. Normalized number $N_{cl,norm}$ of clusters of defective atoms as a function of the temperature T. A nonmonotonic trend is observed, with a maximum at a temperature of about 79 K. The occurrence of the maximum results from the competition between cluster ramification, fragmentation and coalescence processes.[29,30]

The continuous rearrangement of the coordination shells of defective atoms determines a continuous change in the number N_{cl}, the size n and the shape of defective atom clusters, which undergo ramification, fragmentation, and coalescence processes.[29,30] In particular, Figure 2 shows that the number N_{cl} of clusters attains a maximum value at about 79 K. The N_{cl} values reported in Figure 2 have been actually normalized to the total number of atoms considered, i.e., 6912. The normalized number of clusters $N_{cl,norm}$ will be useful for sake of comparison between the cases of homogeneous and heterogeneous melting.

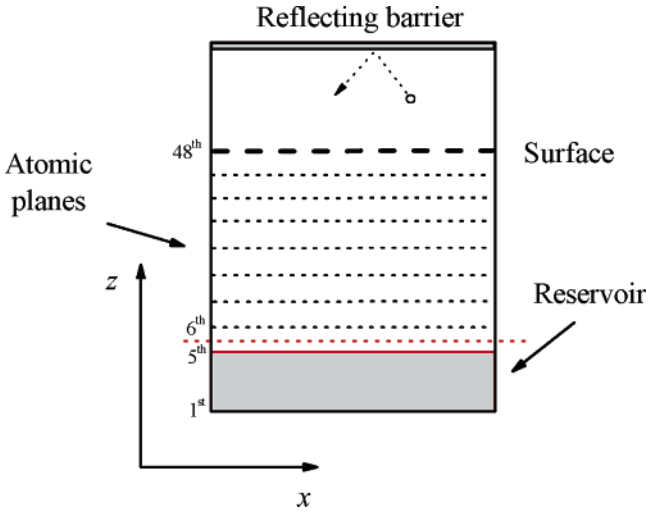

Figure 3. Schematic illustration of the simulation box. The system consists of a stacking of (110) atomic planes terminating with a free plane surface. At the bottom, a reservoir region containing immobile atoms arranged according to a perfect fcc lattice is defined. The horizontal dotted red line separates the 5th atomic plane belonging to the reservoir from the 6th one lying outside the reservoir. At the top, an empty space is available to atomic species moving in the vapor phase. The empty space terminates with a reflecting barrier in order to keep constant the total number of atoms in the system.

IV. Heterogeneous Melting

The mechanism of heterogeneous melting was studied on a semicrystal of 6912 atoms terminating with a free plane surface. To avoid undesired dynamical processes due to the undamped collective motion of the atomic planes close to the free surface, the semicrystal was prepared by starting from a larger system of 8352 atoms. These were arranged in order to have a stacking sequence of 58 (110) atomic planes each of which containing 144 atoms. PBCs were applied only along the *x* and *y* Cartesian directions, while along the *z* one two reservoir regions containing immobile atoms distributed on five atomic planes were defined. The initial configuration was equilibrated for 2×10^4 time steps at a temperature $T = 60$ K and an external pressure $P \approx 0$. The system was subdivided into two regions *A* and *B*. *A* included the atoms contained in the atomic planes from the 1st to the 48th one, and *B* included the remaining species. With the aim of creating a relaxed free surface, the pair interactions between any atom belonging to the *A* region and any other atom belonging to the *B* region were then gradually canceled. This was done by linearly decreasing the energy well depth ϵ to zero in 1000 time steps . A partially relaxed atomic configuration was thus obtained representing the actual initial configuration for the simulation of heterogeneous melting process. Such initial configuration was then further equilibrated according to the procedure already described. In agreement with the typical behavior induced by pair potentials,[33,34] a slight outward relaxation of the atomic planes near the surface was observed.

The relaxed system consisted then of a stacking of 48 (110) atomic planes along the *z* Cartesian direction with PBCs applied along the *x* and *y* Cartesian directions and a reservoir region consisting of five planes of immobile atoms at the bottom of the simulation cell. The top of the simulation cell was instead occupied by an empty space, with a height corresponding to about 10 atomic planes, that permitted the passage of surface atoms from the solid to the vapor phase. For sake of simplicity, the empty space was bounded along the *z* Cartesian direction by a reflective barrier. A schematic illustration of the simulation cell is shown in Figure 3.

The gradual temperature rise induced a modification of structural and thermodynamic properties, including a smooth increase of the fcc elementary cell parameter *a*. Taking into account that the reservoir contains immobile species, a correct simulation of the process of thermal expansion required a proper change of *a* also in the reservoir in order to mimic the behavior of a semi-infinite crystal and avoid unphysical effects. Such change was performed by rescaling *a* at each temperature increase to a value equal to the average one attained in a surface-free bulk at the same temperature.

The decrease of structural order consequent to the increase of the atomic vibration amplitudes as the temperature increases was quantified by means of the planar static order parameter $S_p(\boldsymbol{k})$[9,28,33]. In agreement with previous studies,[35] the sequences of $S_p(\boldsymbol{k})$ values for the 48 atomic planes, not reported here for sake of brevity, indicate that the heterogeneous melting point T_m amounts to about 80 K. The $S_p(\boldsymbol{k})$ values also permitted to characterize the consequences of the evident anisotropy induced along the *z* Cartesian direction by both the reservoir and the free surface. In particular, a comparison between the $S_p(\boldsymbol{k})$ values for the 48 atomic planes of the semicrystal and for a similar stacking in a bulk system at the same temperatures revealed, for example, ordering effects due to the presence of immobile reservoir atoms extending up to the 11th plane.

The highest degree of structural order pertains of course to the atomic plane adjacent to the reservoir and the lowest one to surface planes. Even at 60 K the 47th and 48th atomic planes display $S_p(\boldsymbol{k})$ values of about 0.70, significantly smaller than the ones of about 0.90 observed on the average for the other planes. Such behavior is motivated by the fact that the atoms in the 47th and 48th planes, due to their lower coordination number, can partially intermix and form vacancy−adatom pairs.[33] The rate of these processes increases rapidly with the temperature. The proliferation of vacancies in the 47th and 48th atomic planes, indirectly estimated by evaluating the number of adatoms, is governed by values of the apparent activation energy E_a characteristic of each plane. The E_a values were quantified by quoting in a semilogarithmic plot the number of vacancies in each plane as a function of the inverse of temperature. The obtained E_a values, close to previous estimates,[33] amount approximately to 3.54 kJ mol^{-1} for the 47th atomic plane and to 0.65 kJ mol^{-1} for the 48th plane. Such relatively low values explain the high content of vacancies at the surface even at temperatures significantly lower than T_m.

The formation of vacancies and the associated increase of atomic mobility induce a decrease of the $S_p(\boldsymbol{k})$ values of the surface planes roughly from 0.7 at 60 K to 0.3 at T_m. Taking into account the rough melting criterion according to which a crystalline region melts when $S(\boldsymbol{k})$ is smaller than 0.6, the numerical findings indicate that the surface planes undergo a solid−liquid transition at about 65 K. This evidence suggests, then, the occurrence of premelting phenomena, which remain, however, limited to the surface layer until the equilibrium melting point T_m is attained.

Unless involved in annihilation events, the vacancies belonging to the 47th and 48th planes can undergo migration processes assisted by the local rearrangement of atomic coordination shells induced by thermal vibrations. Although the enhanced mobility of surface atoms facilitates the displacements along the *x* and *y* Cartesian directions, the probability that a vacancy could migrate along the *z* Cartesian direction via a conventional thermal diffusion mechanism increases with the temperature. The fractions c_{vac} of vacant sites per plane at three different temperatures are reported in Figure 4. Profiles typical of

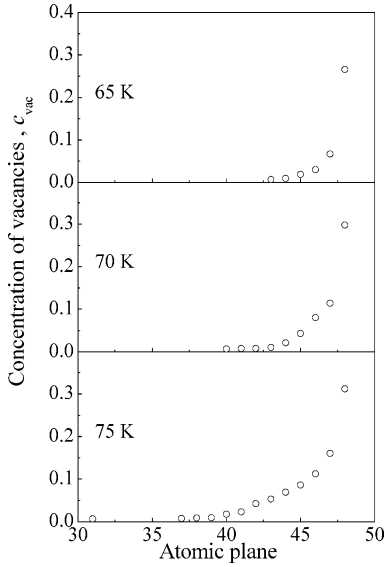

Figure 4. Concentration c_{vac} of vacancies along the z Cartesian direction at the three different temperatures quoted. The concentration decreases as the distance from the free surface increases. The isolate point in correspondence of the 32nd atomic plane at the highest temperature considered indicates the existence of a vacancy originated from the dissociation of a vacancy−interstitial complex.

diffusive processes are observed, with c_{vac} smoothly decreasing along the z Cartesian direction as the distance from the free surface increases. As expected, the number of vacant sites and the depth of the concentration profile increase with the temperature. Even though vacancy−interstitial complexes occasionally appear as a consequence of thermal vibrations, as pointed out by the formation of particular aggregates of 13-fold and 11-fold coordinated atoms, the presence of vacancies in atomic planes relatively far from the surface can be ascribed essentially to migration processes. The percentage of vacancies generated by the dissociation of vacancy−interstitial complexes approximately amounts to only 10%.

The dynamics of vacancies deserves here some comment. The profiles shown in Figure 4 indicate that the surface behaves as a source of vacancies. The concentration of vacancies in the system terminating with the plane surface is significantly larger than the one on the order of 10^{-4} expected according to experimental evidences. Values on the right order of magnitude are actually observed in the surface-free bulk, the concentration of vacancies changing there from about 7×10^{-4} to about 1.2×10^{-3} in the temperature range from T_m to T_m^K. The larger content of vacancies observed in the presence of a free surface is, therefore, a consequence of the surface dynamics. However, if surface planes are neglected and only bulk ones are taken into account the total concentration of vacancies in the semicrystal is not far from the one observed in the surface-free system. It is also worth noting that the total number of vacancies in the semicrystal is significantly affected by size effects. The concentration of vacancies can indeed change up to about the 30% in semicrystals with different surface areas and heights.

The appearance of atoms with defective coordination is at the basis of the formation of vacancies as well as of their migration far from the surface layers and represents an intrinsic aspect of the system dynamics. The fraction $\alpha_d(T)$ of defective atoms can be used as in the case of the surface-free bulk to gain insight into the mechanistic features of the melting process undergone by the semicrystal. In this case, however, the presence of surface atoms with intrinsic defective coordination and of ordering effects extending roughly up to the 11th plane must

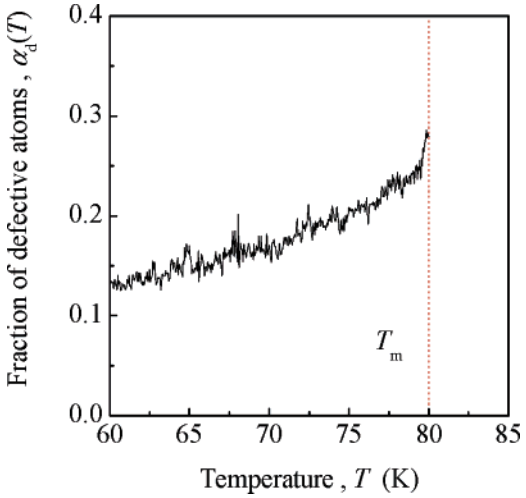

Figure 5. Fraction $\alpha_d(T)$ of defective atoms as a function of the temperature T. The fraction is referred to 5184 atoms. The fraction $\alpha_d(T_m)$ of defective atoms at the equilibrium melting point T_m amounts to only 0.28, a value significantly smaller than the $\alpha_d(T_m^K)$ one of about 0.4 observed in the surface-free bulk at the homogeneous melting point T_m^K.

be taken in due consideration. For these reasons, the process of defective atom formation has been characterized within the crystalline region between the 10th and the 46th atomic planes. The fraction $\alpha_d(T)$ of defective atoms has been correspondingly referred to 5184 atoms. The data reported in Figure 5 point out that $\alpha_d(T)$ increases with the temperature, attaining a value of about 0.28 at T_m. The $\alpha_d(T_m)$ value characterizing the heterogeneous melting is then significantly smaller than the $\alpha_d(T_m^K)$ one of about 0.4 observed in the case of homogeneous melting.

V. Comparison between Homogeneous and Heterogeneous Melting Processes

It is here worth noting that the direct comparison between the two $\alpha_d(T_m)$ and $\alpha_d(T_m^K)$ values is not particularly significant, given that the semicrystal undergoing heterogeneous melting is not as isotropic as the surface-free bulk undergoing homogeneous melting. The anisotropy induced by the presence of the reservoir region and the free surface is indeed expected to result in a nonuniform distribution of defective atoms along the z Cartesian direction. With the aim of suitably investigating this point, the crystalline region of 36 atomic planes considered was then divided into 12 slices of 3 atomic planes each, i.e., of 432 atoms on the average. The distribution of defective atoms along the z Cartesian direction was evaluated by calculating the fractions $\alpha_{d,s}(T)$ of defective atoms in each slice s, defined as the ratio between the number of defective atoms and the total number of atoms in the s-th slice. The $\alpha_{d,s}(T)$ values at three different temperatures are quoted in Figure 6 as a function of the slice number s, which is equal to 1 for the slice closer to the reservoir region and to 12 for the slice below the surface planes. The distribution of the $\alpha_{d,s}(T)$ values along the z Cartesian direction is strongly anisotropic and the fraction $\alpha_{d,12}(T_m)$ of defective atoms in the slice below the surface at the equilibrium melting point T_m amounts to about 0.38. At such temperature, the 12th slice is going to melt, becoming thus the first slice involved in the propagation of the solid−liquid transition front. As the temperature is raised, the static order parameter $S(\boldsymbol{k})$ of the slice drops indeed to values smaller than 0.6. It appears, then, that the slice in which melting is incipient

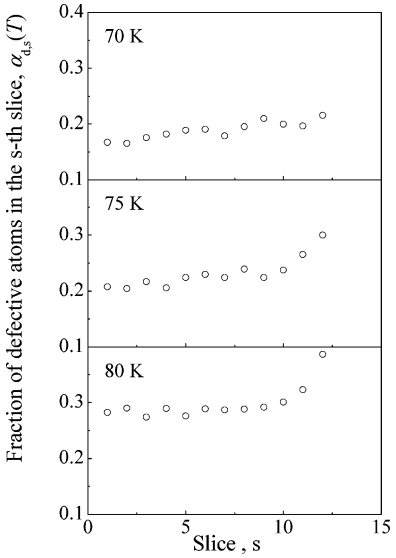

Figure 6. Fraction $\alpha_{d,s}(T)$ of defective atoms as a function of the slice number s at three different temperatures. The slice referred to as 1 is the slice closer to the reservoir region and the 12th one is located immediately below the surface planes. The slices closer to the surface display $\alpha_{d,s}(T)$ values larger than the others. At the equilibrium melting point T_m, the fraction $\alpha_{d,12}(T_m)$ of defective atoms in the 12th slice amounts to about 0.38.

contains a fraction $\alpha_{d,12}(T_m)$ of defective atoms approximately equal to the $\alpha_d(T_m^K)$ one observed in the case of homogeneous melting.

A similar correlation between the fraction $\alpha_{d,s}(T_{m,s})$ of defective atoms in the s-th slice and its melting at $T_{m,s}$ is observed for all the 12 slices. The drop of $S(\boldsymbol{k})$ values below 0.6 in a given slice s becoming involved in the propagation of the solid−liquid interface occurs on the average when the fraction $\alpha_{d,s}(T_{m,s})$ of defective atoms in s-th slice is equal to 0.37 ± 0.015. It is worth noting that the melting points $T_{m,s}$ of the slices s are generally slightly different due to the fact that the propagation of the transition front takes place at a finite rate ω comparable with the rate of temperature rise. The propagation rate ω of the transition front amounts initially to about 4.5 m s^{-1}, but its value increases steadily with the degree of superheating.[9]

As in the case of homogeneous melting, the defective atoms form clusters of variable size and shape. The latter is significantly affected by the presence of either the free surface or the solid−liquid interface. Three defective atom clusters belonging to the atomic configuration at 80.2 K are reported in Figure 7 for sake of illustration. It can be seen that the defective atoms mostly accumulate in the region below the solid−liquid interface. A small number of defective atoms forms however filamentary structures, connected to the main cluster body, roughly extending along the *z* Cartesian direction.

The number and the depth of such filamentary structures vary from cluster to cluster. Such structures are directly involved in the mechanism governing the evolution of the clusters as the solid−liquid interface propagates. It is indeed around such columnar structures that additional defective atoms appear as the molten phase approaches. This fact and the evidence that a relatively large number of defective atoms is located below the solid−liquid interface suggest that the number N_{cl} of clusters should be in this case lower than in the case of homogeneous melting. The accumulation of defective atoms in a relatively small interfacial region as well as the connection between columnar structures below the clusters and the appearance of other defective atoms favor indeed the occurrence of cluster coalescence events. Such hypothesis is actually confirmed by the plot of the normalized number $N_{cl,norm}$ of clusters as a function of the temperature T reported in Figure 8. $N_{cl,norm}$ expresses here the total number N_{cl} of clusters in the region between the 10th and the 46th atomic planes normalized to the 5184 atoms therein contained. A comparison of the relevant data in Figure 8 reveals that the $N_{cl,norm}$ values obtained in this case are always smaller than the ones obtained in the case of homogeneous melting.

VI. Discussion

The results discussed above define a complex conceptual framework. Homogeneous and heterogeneous melting processes are governed by different atomic-scale mechanisms. In the former case, the solid−liquid transition consists of a sudden collapse of the crystalline lattice involving at once the whole volume of solid phase. On the contrary, heterogeneous melting is characterized by a marked spatial localization of the processes responsible for the failure of the crystalline phase. A definite transition front propagating from the free surface to the rest of the crystal can be indeed clearly observed. The dynamics of surface atoms plays an essential role. A considerable structural disordering of the surface occurs at temperatures below the equilibrium melting point T_m, resulting in the formation of vacancies and relatively fast diffusion processes that could be in principle interpreted as due to a premelting of the surface layers. The formation and the migration of vacancies far from the surface according to thermal diffusion as well as the thermal disordering of the crystalline lattice are deeply connected with the formation of atoms with defective coordination.

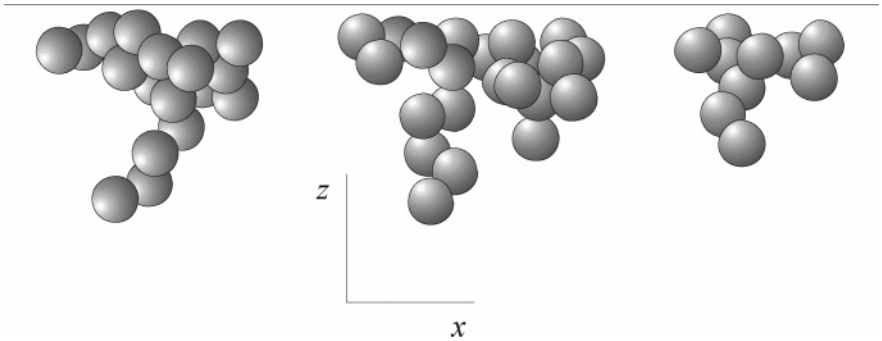

Figure 7. Three different clusters of defective atoms belonging to the atomic configuration at 80.2 K. From left to right, clusters consist of 20, 26, and 11 defective atoms, respectively. For sake of illustration, the figure does not reproduce the original relative positions of the clusters. The largest fraction of defective atoms forming the cluster is located immediately below the solid−liquid interface, the position of which is indicated by the dashed horizontal line. Filamentary sub-aggregates of defective atoms extending along the *z* Cartesian direction are visible below the clusters.

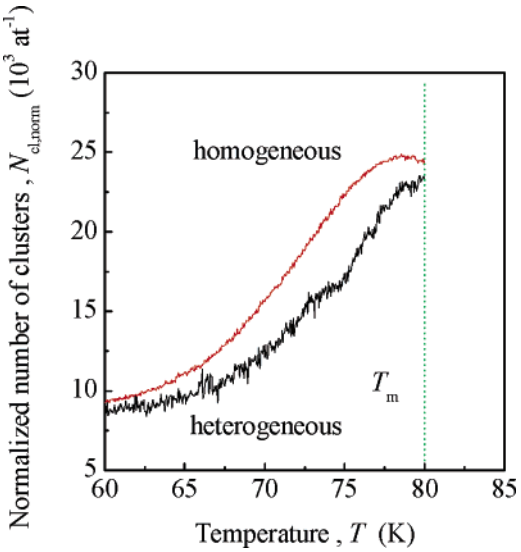

Figure 8. Normalized number $N_{cl,norm}$ of clusters of defective atoms as a function of the temperature T. The $N_{cl,norm}$ data obtained in the case of homogeneous melting have been also quoted for sake of comparison. In both cases, $N_{cl,norm}$ undergoes a monotonic increase. Temperature being equal, the $N_{cl,norm}$ values for heterogeneous melting have values slightly smaller than the ones for homogeneous melting. This is the consequence of the facilitated cluster coalescence processes involving the defective atom aggregates at the surface. The fluctuations affecting the $N_{cl,norm}$ values for heterogeneous melting are also larger than for homogeneous melting, due to the dynamics of surface species that induces significant oscillations in the total number of defective atoms.

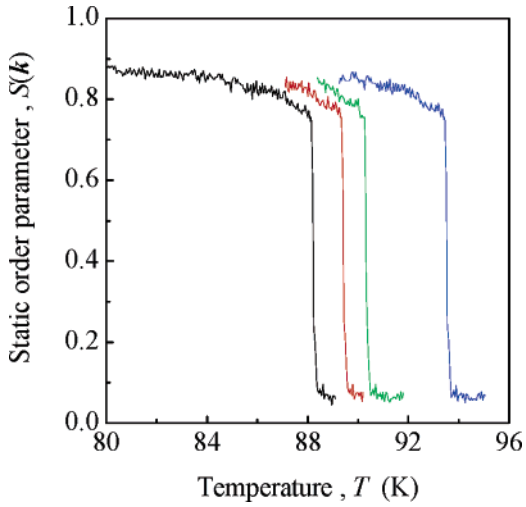

Figure 9. Values of the static order parameter $S(\boldsymbol{k})$ for the systems with a different initial content of vacancies as a function of temperature T. From left to right, the four curves refer to systems with 120, 100, 80, and 0 vacancies, respectively. It can be seen that the homogeneous melting point T_m^K at which $S(\boldsymbol{k})$ suddenly drops depends on the total number of vacancies in the system.

The formation of defective atoms appears to be the only common feature shared by homogeneous and heterogeneous melting processes, even though the fraction of defective atoms involved, the total number of defective atom clusters, and their shape are significantly different. However, an interesting connection between the mechanisms of homogeneous and heterogeneous melting is provided by the evidence that the fraction of defective atoms in the region of the semicrystal immediately below the solid−liquid interface at the melting point is approximately equal to the fraction of defective atoms in the surface-free bulk at the limit of superheating. This suggests that the failure of a certain volume of crystalline lattice is related to the attainment within such volume of a critical concentration of defective atoms.

With the aim of further investigating the role of both vacancies and defective atoms in the onset of the melting process, additional numerical simulations were carried out to study how an initial content of vacancies, and then of defective atoms, affects the thermal behavior of a surface-free bulk. Starting from an atomic configuration relaxed at 60 K and zero pressure, a certain number of vacancies was introduced in the system of 6912 atoms closed by PCBs along the three Cartesian directions. In a first series of simulations, the vacancies were introduced randomly in order to obtain a uniform distribution in the system. In a second series of calculations, the vacancies were instead created only in the slice of four (100) atomic planes approximately at the center of the simulation box along the z Cartesian direction. In all the cases, after the removal of atoms the system was relaxed for 2500 times steps. The temperature was then increased at the same nominal heating rate previously employed. Each additional simulation was repeated at least once to sample different initial configurations. It is worth noting that these simulations represent idealized situations in which the number of vacancies is decided a priori irrespective of any thermal mechanism. The concentration of vacancies is thus considerably larger than the equilibrium one. Far from being representative of experimental situations, the calculations are instead only aimed to ascertain the role of an initial content of defective atoms, or alternatively, of vacancies, in the onset of the homogeneous melting process in a surface-free crystalline region.

In the first series of calculations the number n_v of vacancies introduced in the system was equal to 80, 100, and 120, respectively. The fraction $\alpha_d(T)$ of defective atoms correspondingly generated was 0.14, 0.17, and 0.21, being each vacancy surrounded by twelve nearest neighbors with 11-fold coordination. At relatively low temperatures, the vacancies undergo low-rate migration processes with the usual thermal diffusion mechanism. The rate of such processes increases with the temperature and is favored by the contemporary increase of the fraction $\alpha_d(T)$ of defective atoms. The static order parameter $S(\boldsymbol{k})$ values for the systems with a different initial content of vacancies, reported in Figure 9 as a function of temperature T, clearly indicate that they have different homogeneous melting points T_m^K. As shown in Figure 10, T_m^K displays in particular a roughly linear dependence on the number n_v of vacancies. The fraction $\alpha_d(T_m^K)$ of defective atoms at the homogeneous melting point T_m^K is instead approximately the same for all the systems and amounts to about 0.39 ± 0.03. The number of vacancies in the system affects, therefore, the homogeneous melting point T_m^K, but $\alpha_d(T_m^K)$ is always equal to about 0.4. It is also worth noting that the onset of the melting process is not related to the content of vacancies. Even though the latter is remarkably higher than the equilibrium one, melting only occurs when the content of defective atoms attains a certain value. The failure of the crystalline lattice, therefore, is governed by the total number of defectively coordinated atoms and not by vacancies.

The second series of calculations with a nonuniform distribution of vacancies was aimed to study the effect of a significant structural heterogeneity on the system thermal behavior. Computations were carried out on two systems containing in the central slice of four (100) atomic planes, respectively, 20 and 40 vacancies. The creation of vacancies in the central slice by a random removal of atoms was followed by an equilibration

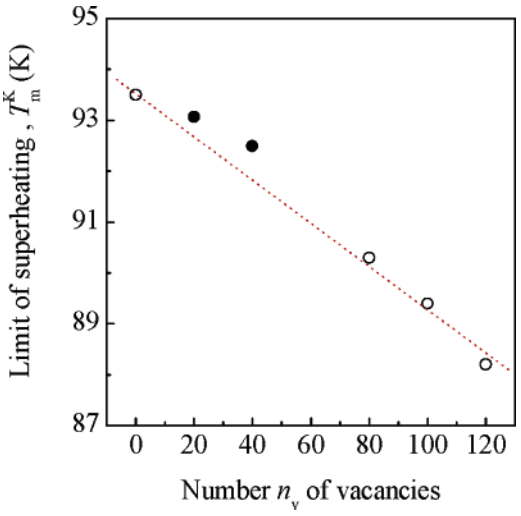

Figure 10. Homogeneous melting point T_m^K () as a function of the number n_v of vacancies in the system. A roughly linear decrease of the T_m^K as n_v increases is observed. The best fitted line is shown. For sake of comparison, the homogeneous melting points T_m^K (˜) obtained when the vacancies were randomly distributed within the central slice of four (100) atomic planes are also shown. Also in this case T_m^K decreases as n_v increases.

stage of 2500 time steps, after which the temperature was gradually increased. Due to the high local concentration of vacancies, the central slice is characterized by the occurrence of a relatively fast rearrangement of atomic positions. Whenever vacancies are able to migrate independently from each other, their distribution in the system volume becomes gradually more uniform as a result of the diffusion processes. Thermal processes also determine a gradual increase of the number of defective atoms as the temperature increases and the melting takes place when $\alpha_d(T_m^K)$ amounts approximately to 0.38 ± 0.01. This occurs at slightly different temperatures T_m^K, also reported in Figure 10.

In all the cases discussed above, the mechanism of melting remained essentially homogeneous. However, in one of the simulations with 40 vacancies in the central slice, a heterogeneous melting mechanism was observed. The reason lies in the fact that six vacancies came into contact after about 25 000 time steps as a result of thermal diffusion events. This determined the formation of a nanometer-sized void approximately at the center of the simulation box. The void, a section of which is reported in Figure 11 for sake of illustration, remained stable during the simulation run although the gradual temperature rise induced an increase of the atomic mobility. The so-called Lindemann parameter δ_r,[11,22] defined as the ratio between the root-mean-square displacement of atoms[28] and the average nearest-neighbors distance, was used to quantify the thermal displacements from equilibrium lattice positions. At any given temperature, the largest δ_r values were seen to pertain to the atoms surrounding the nanometer-sized void. Following previous work,[11] δ_r values greater than 0.22 were regarded as characteristic of the molten phase. The snapshot of atoms with δ_r greater than 0.22 at 85.5 K, shown in Figure 12 for sake of illustration, clearly shows that melting first involves the atoms surrounding the void. The latter undergoes marked fluctuations in shape, but is still distinguishable up to about 86 K. At such temperature, a local failure of the lattice takes place and a first nucleus of molten phase is formed determining the disappearance of the void. The melting process observed displays clear heterogeneous features even though the temperature of 86 K at which it occurs is significantly higher than the equilibrium melting point T_m of about 80 K estimated in the presence of a free plane surface. It is finally worth noting that the fraction $\alpha_d(T_m)$ of defective atoms at the melting point of 86 K roughly amounts to 0.37. Once more, therefore, the failure of the crystalline lattice occurs when $\alpha_d(T)$ attains a value close to 0.4.

All the evidences hitherto discussed suggest that the occurrence of a melting process either under equilibrium conditions or at the limit of superheating is associated with a critical fraction of atoms characterized by a defective coordination. Despite the important differences in the atomic scale mechanisms governing the onset of the lattice instability, the nucleation of the molten phase seems to be intimately related to the formation of defective atom clusters. Although the fundamental reasons of the collapse of the crystalline structure still remain obscure, it appears that defective atoms and their aggregates play an essential role in the processes responsible for the onset of melting.

VII. Conclusions

Homogeneous melting at the limit of superheating is associated with the cooperative appearance of atoms with defective coordination. Their uniform distribution and relatively high mobility provide a rationale for the failure of the ordered lattice, which is not able to withstand collective atomic motions above a certain temperature. The heterogeneous transition at the equilibrium melting point onsets instead at the surface, where atomic species have an intrinsic defective coordination and correspondingly a high mobility. The solid−liquid transition front propagates then perpendicularly to the surface, involving

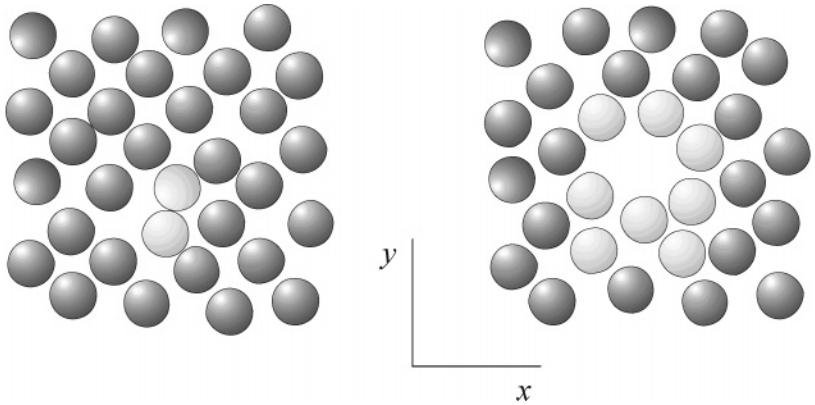

Figure 11. Snapshot of the (100) atomic plane containing the nanometer-sized void (right panel). For sake of comparison, a snapshot of a (100) atomic plane not involved in the formation of the void is also reported (left panel). In both cases, light gray is used to indicate defective atoms. Dark gray atoms have indeed a normal coordination. The atomic configurations shown refer to a temperature of 70 K.

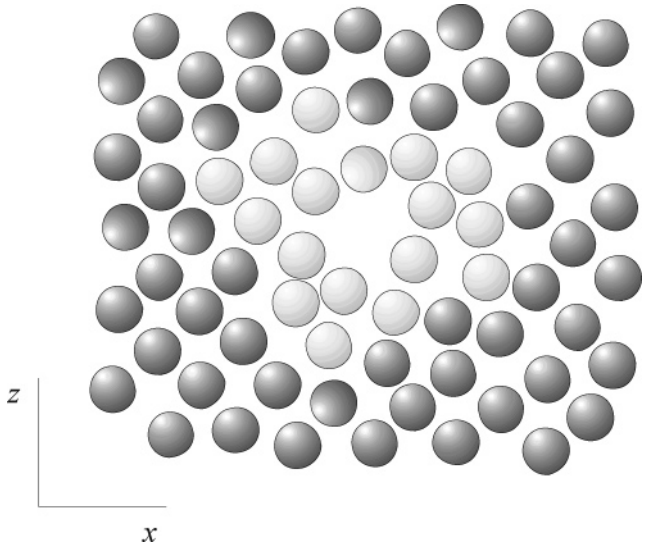

Figure 12. Snapshot of the (100) atomic plane containing the nanometer-sized void at 85.5 K. The atoms with Lindemann parameter δ_r greater than 0.22 are shown in light gray. These can be regarded as belonging to a molten phase. According to such criterion, the void is completely surrounded by a liquidlike layer.

successive atomic layers. This process is governed by the formation and migration of vacancies as well as of atoms with defective coordination.

The differences in average global quantities such as the concentration of vacancies, the fraction of defective atoms and the number of their clusters suggest that homogeneous and heterogeneous melting processes take place according to different mechanisms. They appear however intimately connected when attention is focused on local quantities, i.e., quantities averaged only over the region directly involved in the structural collapse. In the case of homogeneous melting such region corresponds to the whole system volume, so that global and local averages are roughly equivalent. Conversely, the heterogeneous melting is a highly localized process taking place within the transition front region consisting of a few atomic planes. The local quantities evaluated over such small region are significantly different from the global ones averaged over the whole volume. In particular, the local fraction of defective atoms is roughly equal to the one observed in the case of homogeneous melting. This evidence represents a first indication of the deep similarity of the atomistic processes underlying both the homogeneous and heterogeneous melting processes.

Acknowledgment. Dr. L. Burakovsky, Theoretical Division, Los Alamos National Laboratory, Los Alamos, U.S.A., is gratefully acknowledged for stimulating discussions. Prof. G. Cocco, Department of Chemistry, University of Sassari, Italy, and dr. G. Manai, Department of Physics, Trinity College, Dublin, Ireland, are gratefully acknowledged for useful suggestions. A. Ermini, ExtraInformatica s.r.l., is gratefully acknowledged for technical support. Financial support was given by the University of Cagliari.

References and Notes

(1) Dash, J. G. *Contemp. Phys.* **2002**, *43*, 427.
(2) Cormia, R. L.; Mackenzie, J. D.; Turnbull, D. *J. Appl. Phys.* **1963**, *34*, 2239.
(3) Cahn, R. W. *Nature* **1986**, *323*, 668.
(4) Maddox, J. *Nature* **1987**, *330*, 599.
(5) Daeges, J., Gleiter, H., Perepezko, J. H. *Phys. Lett. A* **1986**, *119*, 79.
(6) Zhang, D. L., Cantor, B. *Acta Metall. Mater.* **1991**, *39*, 1595.
(7) Lindemann, F. A. *Z. Phys.* **1910**, *11*, 609.
(8) Born, M. *J. Chem. Phys.* **1939**, *7*, 591.
(9) Wolf, D.; Okamoto, P. R.; Yip, S.; Lutsko, J. F.; Kluge, M. *J. Mater. Res.* **1990**, *5*, 286.
(10) Lu, K., Li, Y. *Phys. Rev. Lett.* **1998**, *80,* 4474.
(11) Jin, Z. H.; Gumbsch, P.; Lu, K.; Ma, E. *Phys. Rev. Lett.* **2001**, *87*, 055703.
(12) Cahn, R. W. *Nature* **2001**, *413*, 582.
(13) Belonoshko, A. B.; Skorodumova, N. V.; Rosengren, A.; Johansson, B. *Phys. Rev. B* **2006**, *73* 012201.
(14) Tallon, J. L. *Nature* **1989**, *342*, 658.
(15) Kosterlitz, J. M.; Thouless, D. J. *J. Phys. C* **1973**, *6*, 1181.
(16) Nelson, D. R.; Halperin, B. I. *Phys. Rev. B* **1979**, *19*, 2457.
(17) Young, A. P. *Phys. Rev. B* **1979**, *19*, 1855.
(18) Chen, K.; Kaplan, T.; Mostoller, M. *Phys. Rev. Lett.* **1995**, *74*, 4019.
(19) Chou, C. F.; Jin, A. J.; Hui, S. W.; Huang, C. C.; Ho, J. T. *Science* **1998**, *280*, 1424.
(20) Zahn, K.; Maret, G. *Phys. Rev. Lett.* **2000**, *86*, 3656.
(21) Zangi, R.; Rice, S. A. *Phys. Rev. Lett.* **2004**, *92*, 035502.
(22) Kleinert, H. *Gauge Theory in Condensed Matter;* World Scientific: Singapore, 1989.
(23) Burakovsky, L.; Preston, D. L.; Silbar, R. R. *Phys. Rev. B* **2000**, *61*, 15011.
(24) Gomez, L.; Dobry, A.; Geuting, Ch.; Diep, H. T.; Burakovsky, L. *Phys. Rev. Lett.* **2003**, *90*, 095701
(25) Andersen, H. C. *J. Chem. Phys.* **1980**, *72*, 2384.
(26) Nosè, S. *J. Chem. Phys.* **1984**, *81*, 511.
(27) Parrinello, M.; Rahman, A. *J. Appl. Phys.* **1981**, *52*, 7182.
(28) Allen, M. P.; Tildesley, D. *Computer Simulation of Liquids;* Clarendon Press: Oxford, 1987.
(29) Delogu, F. *J. Phys. Chem. B* **2005**, *109*, 20295.
(30) Delogu, F. *J. Phys. Chem. B* **2006**, *110*, 3281.
(31) Braunstein, L. A.; Buldyrev, S. V.; Havlin, S.; Stanley, H. E. *Phys. Rev. E* **2002**, *65*, 056128.
(32) Honeycutt, J. D.; Andersen, H. C. *J. Phys. Chem.* **1987**, *91*, 4950.
(33) Rosato, V.; Ciccotti, G.; Pontikis, V. *Phys. Rev. B* **1986**, *33*, 1860.
(34) Gupta, R. P. *Phys. Rev. B* **1981**, *23*, 6265.
(35) Broughton, J. Q.; Gilmer, G. H. *Phys. Rev. Lett.* **1986**, *56*, 2692.